

PHASEAUG: A DIFFERENTIABLE AUGMENTATION FOR SPEECH SYNTHESIS TO SIMULATE ONE-TO-MANY MAPPING

Junhyeok Lee¹ Seungu Han^{2,4*} Hyunjae Cho^{1,2} Wonbin Jung^{1,3}

¹ MINDsLab Inc., Republic of Korea

² Seoul National University (SNU), Republic of Korea

³ Korea Advanced Institute of Science and Technology (KAIST), Republic of Korea,

⁴ Supertone Inc., Republic of Korea

ABSTRACT

Previous generative adversarial network (GAN)-based neural vocoders are trained to reconstruct the exact ground truth waveform from the paired mel-spectrogram and do not consider the one-to-many relationship of speech synthesis. This conventional training causes overfitting for both the discriminators and the generator, leading to the periodicity artifacts in the generated audio signal. In this work, we present PhaseAug, the first differentiable augmentation for speech synthesis that rotates the phase of each frequency bin to simulate one-to-many mapping. With our proposed method, we outperform baselines without any architecture modification. Code and audio samples will be available at <https://github.com/minds-lab/phaseaug>.

Index Terms— speech synthesis, neural vocoder, differentiable augmentation, phase, generative adversarial networks

1. INTRODUCTION

Neural vocoder synthesizes raw audio waveform from input acoustic feature, such as mel-spectrogram or latent variable. While a variety of generative models are applied to vocoder task, generative adversarial networks (GANs) [1] are the most commonly used generative models for vocoder task [2, 3, 4, 5, 6, 7, 8]. GAN-based vocoder models after MelGAN [2] are mainly focused on modifying GAN architectures, among these, HiFi-GAN [4] utilizes two kinds of raw waveform discriminators, multi-scale discriminators (MSD) and multi-period discriminators (MPD), to achieve a state-of-the-art GAN-based non-autoregressive vocoder. However, during training HiFi-GAN, we observed training accuracies of MSD and MPD converged to 100% and over 70% respectively, which indicates discriminator overfitting.

For GAN-based image synthesis, discriminator training methods are being actively studied, such as differentiable augmentation (DiffAugment) [9] and adaptive discriminator augmentation (ADA) [10]. These methods apply DiffAugment

to real data and generated output to prevent overfitting of the discriminator and to provide useful gradients for the generator. While there are speech synthesis studies adapting data augmentations [11, 12, 13], there are no speech synthesis studies adapting DiffAugment to GAN to the best of our knowledge.

GAN-based non-autoregressive vocoders also suffer from a one-to-one paired data problem. While neural vocoding is a one-to-many mapping problem, previous neural vocoders were trained assuming a one-to-one mapping between the ground truth waveforms and the paired mel-spectrograms. Recently, Morrison *et al.* [6] claim that non-autoregressive generators of vocoders are forced to generate the exact phases of ground truth signal from the mel-spectrogram without providing the initial phase. In addition, Morrison *et al.* [6] report that HiFi-GAN generates the perceptible periodicity artifact and suggest periodicity error, which is extracted from the pitch estimation model CREPE [14], to measure it. We hypothesize that the periodicity artifact is related to a one-to-one paired data training, since generators are overfitted to generate a given phase of each ground truth waveform.

To overcome the discriminator overfitting and the one-to-one paired data problem, we propose *PhaseAug*, the first differentiable augmentation for audio signal synthesis, to simulate one-to-many mapping by rotating signal’s phases on the frequency domain. Compared to conventional trained HiFi-GAN and MelGAN, we outperform each of the models by simply applying PhaseAug to these models.

2. PHASEAUG

2.1. Fourier Transformation

In the signal processing domain, Fourier transformation is widely applied to analyze time-series signals in the frequency domain. For a real-valued discrete-time digital signal $\mathbf{x} = [x[n]]_{n \in \mathbb{Z}}$, short-time Fourier transform (STFT) \mathcal{F} and inverse short-time Fourier transform (iSTFT) \mathcal{F}^{-1} are represented as:

$$\mathbf{X}[k, m] = \mathcal{F}(\mathbf{x}) = \sum_{n=-\infty}^{\infty} x[n]w[n - md]e^{-j2\pi nk/N}, \quad (1)$$

This work was supported by Institute for Information & communications Technology Planning & Evaluation(IITP) grant funded by the Korea government(MSTI) (No. 2021-0-00062-002, Development of joint work automation management software technology based on task awareness)

* Work performed at MINDsLab Inc.

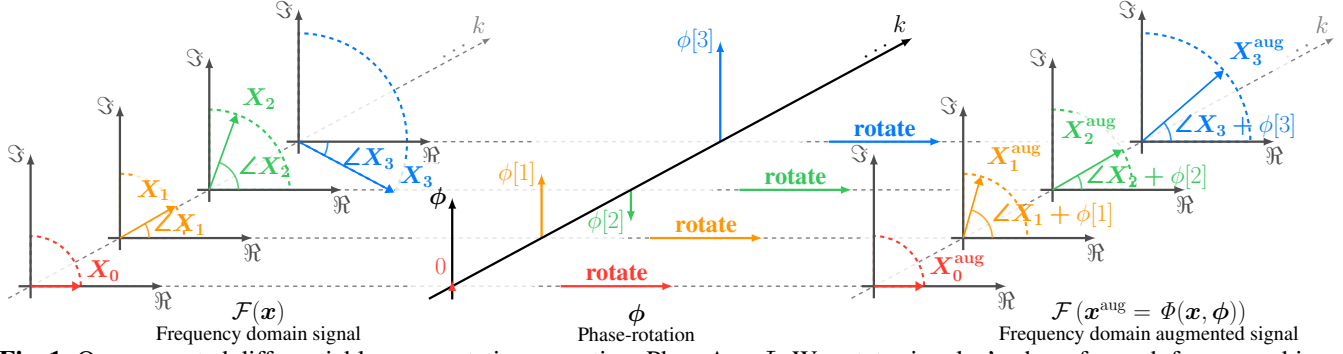


Fig. 1. Our suggested differentiable augmentation operation, PhaseAug Φ . We rotate signal x 's phase for each frequency bin as ϕ to generate augmented signal x^{aug} . X_k for $0 \leq k \leq N/2$ are abbreviation of $X[k, m]$ for arbitrary m th time frame.

$$x[n] = \mathcal{F}^{-1}(X[k, m]) = \frac{1}{C} \sum_{k=0}^{N-1} \sum_{m=-\infty}^{\infty} X[k, m] e^{j2\pi nk/N}, \quad (2)$$

where N is the size of STFT, d is the hop size, $[k, m]$ are the respective frequency bin and time frame indices of Fourier feature \mathbf{X} , $w[n]$ is the Hann-window $w[n] = (1 - \cos(2\pi n/N))/2$ for $0 \leq n \leq N-1$ else 0, and $C = \sum_{m=-\infty}^{\infty} w[n - md]$ is the overlap-add value of Hann-window. Since real-valued x satisfies $X[k, m] = X[N-k, m]^*$, $\forall k \in \mathbb{Z}$, we can consider a one-sided STFT in $0 \leq k \leq N/2$ as $X[k, m] \in \mathbb{C}^{(N/2+1) \times M}$. We start all vector and matrix indices at 0, since the range of k starts at 0. From the definition, STFT of $x[n - \delta]$, for a small enough time-shift $\delta \ll N$ on signal $x[n]$, can be approximated as:

$$\begin{aligned} \mathcal{F}(x[n - \delta]) &= \sum_{n=-\infty}^{\infty} x[n - \delta] w[n - md] e^{-j2\pi nk/N} \\ &\approx X[k, m] e^{-j2\pi \delta k/N}, \end{aligned} \quad (3)$$

since difference of window is negligible for small enough δ .

2.2. PhaseAug

The one-to-many relationship between mel-spectrogram and raw waveform is not considered by previous studies, thus vocoders were forced to generate exact ground truth waveforms. We present *PhaseAug* which arbitrarily rotates the phase of each frequency bin without manipulating magnitude to simulate one-to-many mapping from paired data. We define PhaseAug operation Φ as:

$$\Phi(x, \phi) = \mathcal{F}^{-1}(\text{diag}(e^{j\phi}) \mathcal{F}(x)), \quad (4)$$

where $\phi = [0 \ \phi[1] \ \phi[2] \ \dots \ \phi[N/2]] \in \mathbb{R}^{(N/2+1)}$ is a vector of phase-rotation for each frequency bin in radian, and $\text{diag} : \mathbb{C}^{(N/2+1)} \rightarrow \mathbb{C}^{(N/2+1) \times (N/2+1)}$ denotes vector-to-matrix operator that maps elements of the vector to the main diagonal elements of a square diagonal matrix. From (3), PhaseAug operation is identical to rotating the phase of k th

frequency bin as $\phi[k]$ without modifying the magnitude and the relative phase between the adjacent time frames. We always set $\phi[0] = 0$ to prevent DC offset and complex output. Since all of the components, including STFT and iSTFT, are differentiable, PhaseAug is applicable as DiffAugment [9]. We expect that PhaseAug could reduce the periodicity artifacts by preventing the discriminators and the generator from overfitting to the ground truth phase.

From (3) and (4), time-shifted signal $x[n - \delta]$, where $\delta \in \mathbb{Z}$, can be approximated by PhaseAug as:

$$x[n - \delta] \approx \Phi(x[n], -\delta\phi_{\text{ref}}), \quad (5)$$

where $\phi_{\text{ref}} = 2\pi/N \cdot [0 \ 1 \ 2 \ \dots \ N/2]$ is a reference phase-rotation vector. With PhaseAug, time-shift can be approximated as a continuous and differentiable operation by controlling the time-shift value $\delta \in \mathbb{R}$, thus we can generate approximated non-integer time-shifted signal by calculating $\Phi(x, -\delta\phi_{\text{ref}})$. In Fig. 2, we demonstrate that PhaseAug can approximate continuous and differentiable time-shift.

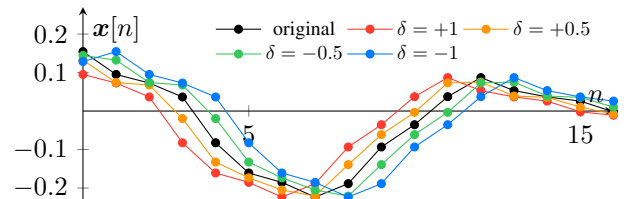


Fig. 2. Plot of original speech signal $x[n]$ (black) and approximated time-shifted signals $\Phi(x, \delta\phi_{\text{ref}})$ by PhaseAug with $\delta = +1$ (red), $+0.5$ (orange), -0.5 (green), and -1 (blue).

For random augmentation, we first attempted to sample phase-rotation μ from $\mu \sim \mathcal{N}(\delta\phi_{\text{ref}}, \sigma^2 \mathbf{I})$ and augmented signal as $x^{\text{aug}} = \Phi(x, \mu)$, but rotating phases by the same variance affects each frequency bin differently. Since $\mu \odot \phi_{\text{ref}}^{-1}$ is shifted time for each frequency bin by (5), where $\phi_{\text{ref}}^{-1} = [0 \ 1/\phi_{\text{ref}}[1] \ 1/\phi_{\text{ref}}[2] \ \dots \ 1/\phi_{\text{ref}}[N/2]]$ and \odot is element-wise multiplication, low-frequency bins are more shifted in time than high-frequency bins. To calibrate variances of frequency bins in the time domain, we consider

$\boldsymbol{\mu} \sim \mathcal{N}(\delta \mathbf{1}, \sigma^2 \mathbf{I})$ as a time-shift for each frequency bin instead of phase-rotation by calculating $\mathbf{x}^{\text{aug}} = \Phi(\mathbf{x}, \boldsymbol{\mu} \odot \boldsymbol{\phi}_{\text{ref}})$. In addition, we observed that \mathbf{x}^{aug} has noticeable distortion with $\boldsymbol{\mu} \sim \mathcal{N}(\delta \mathbf{1}, \sigma^2 \mathbf{I})$. Since Karras *et al.* [10] state that leaking of augmentation has occurred and we also noticed it with the setting above, we attempted to reduce the distortion. We empirically found that a large time-shift difference between adjacent frequency bins occurs in distortion and high-frequency elements in $\boldsymbol{\mu}$ cause a large difference between adjacent frequency bins. To reduce perceptible distortion by removing high-frequency components, we apply a low-pass filter (LPF) to calculate filtered time-shift $\boldsymbol{\mu}_l = \text{LPF}(\boldsymbol{\mu})$, specifically the Kaiser-windowed sinc filter. Moreover, we set $\boldsymbol{\mu}$'s variance $\sigma^2 > 5.2$ to keep the variance of $\boldsymbol{\mu}_l$ greater than 0.5 since LPF in our setup reduces variance by 90.3%. Fig. 3 illustrates the original signal and its random phase-rotated versions which are indistinguishable by hearing.

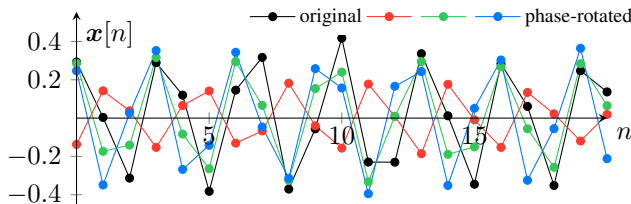


Fig. 3. Plot of original speech signal $x[n]$ (black) and phase-rotated signals $\Phi(x, \phi)$ by PhaseAug with augmentation policy with fixed mean time-shift as $\delta = 0$ (red, green, blue).

2.3. Augmentation Policy

For random augmentation, we apply the following Algorithm 1 to real and generated signals.

Algorithm 1 PhaseAug augmentation policy

Input: signal \mathbf{x}

Output: augmented signal \mathbf{x}^{aug}

- 1: Sample $\delta \sim \mathcal{U}(-\delta_{\text{max}}, \delta_{\text{max}})$
 - 2: Sample $\boldsymbol{\mu} \sim \mathcal{N}(\delta \mathbf{1}, \sigma^2 \mathbf{I})$
 - 3: Compute $\boldsymbol{\mu}_l \leftarrow \text{LPF}(\boldsymbol{\mu})$
 - 4: Compute $\boldsymbol{\phi} \leftarrow \boldsymbol{\mu}_l \odot \boldsymbol{\phi}_{\text{ref}}$
 - 5: Compute $\mathbf{x}^{\text{aug}} \leftarrow \Phi(\mathbf{x}, \boldsymbol{\phi})$
-

2.4. Differentiable Augmentation for GAN-based Vocoder

Since GAN-based vocoders are adopting feature matching loss, we apply PhaseAug with identical $\boldsymbol{\phi}$ to real and generated samples. For paired raw waveform \mathbf{x} and mel-spectrogram \mathbf{s} , the discriminators take the inputs as $\Phi(\mathbf{x}, \boldsymbol{\phi})$ and $\Phi(G(\mathbf{s}), \boldsymbol{\phi})$, where G is the generator model. For a sample, we employ the same phase-rotation $\boldsymbol{\phi}$ to all discriminators due to computational efficiency. In addition, we sample different $\boldsymbol{\phi}$ between discriminators update and generator update for provid-

ing more points of view of waveforms. Mel-spectrogram loss is calculated between \mathbf{x} and $G(\mathbf{s})$, not between $\Phi(\mathbf{x}, \boldsymbol{\phi})$ and $\Phi(G(\mathbf{s}), \boldsymbol{\phi})$.

2.5. Implementation Details

We use one-sided STFT with $N = 1024$ and $d = 256$. We employ Kaiser-windowed sinc kernel with kernel size 128, cut-off frequency of 0.05, and transition band half-width 0.012 for the LPF, and LPF in Algorithm 1 denotes 1D convolution with the specified kernel. We sample B different $\boldsymbol{\phi}$ per step, where B is the batch size during training. We calculate complex tensor as real-valued length 2 vector and multiplying $e^{j\phi[k]}$ is replaced by multiplying rotation matrix $\begin{pmatrix} \cos \phi[k] & -\sin \phi[k] \\ \sin \phi[k] & \cos \phi[k] \end{pmatrix}$. Since time-shift with small enough δ does not cause perceivable artifacts, we set the maximum value for δ to $\delta_{\text{max}} = 2$ which is small enough than N to maintain the mel-spectrogram condition. In the same manner, we set $\sigma^2 = 6$ to get $\boldsymbol{\mu}_l$ with variance approximately 0.58. PhaseAug is applied with 100% augmentation probability with identical augmentation strength. We do not employ ADA [10], since the augmentation probability converged to 100% in every setup of our initial experiments.

3. EXPERIMENTS

3.1. Baselines

To evaluate PhaseAug, we train HiFi-GAN [4], which is a state-of-the-art GAN-based neural vocoder model. In addition, we simply replace the HiFi-GAN generator to the Mel-GAN generator [2] without changing other setups such as mel-spectrogram loss, loss coefficients, MPD, *etc.* for generator architecture ablation. During the training, we follow all configurations, with exception of PhaseAug and size of the dataset, as the official HiFi-GAN V1 configurations. All models are trained from scratch on a V100 GPU.

3.2. Dataset

We trained all models on LJSpeech [15], which contains 24 hours of single-speaker speeches, and divided the training set and the validation set as official HiFi-GAN configurations. Since it contains sufficient amount of files to train vocoder models, we conduct training with 100%, 10%, and 1% of the dataset to evaluate the effect of PhaseAug on various sizes of the dataset including limited data conditions. We take each percentage depending on the number of files and not on the total playtime due to the different playtime of each file. 100% and 10% models are trained until 2.5M steps and 1% models are stopped before their validation mel-spectrogram errors diverge ($\leq 100k$ steps). For limited data size conditions, we choose a model with the minimum validation mel-spectrogram mean average error. In addition, we report means and standard deviations over 3 trainings for evaluation metrics of 1% models, because of there high variance.

Table 1. The evaluation results for models with and without PhaseAug. The bold numbers indicate the better value between with and without PhaseAug. Paired bold numbers indicate that standard deviation or confidence interval ranges are overlapped.

Model	MAE (\downarrow)	M-STFT (\downarrow)	PESQ (\uparrow)	MCD (\downarrow)	V/UV F1 (\uparrow)	Periodicity (\downarrow)	MOS (\uparrow)	Pairwise (\uparrow)
Ground Truth	—	—	—	—	—	—	4.08 ± 0.05	—
+ PhaseAug	0.02368	0.2585	4.608	0.1740	0.9949	0.02062	4.03 ± 0.06	—
HiFi-GAN (100%)	0.2227	1.004	3.634	1.012	0.9582	0.1111	3.91 ± 0.06	32.9%
+ PhaseAug	0.2111	1.001	3.667	1.012	0.9603	0.1053	3.99 ± 0.05	38.1%
MelGAN (100%)	0.2849	1.115	2.924	1.154	0.9477	0.1325	3.98 ± 0.06	32.9%
+ PhaseAug	0.2651	1.091	3.037	1.081	0.9503	0.1270	3.96 ± 0.06	39.7%
HiFi-GAN (10%)	0.2395	1.033	3.494	1.104	0.9543	0.1169	3.97 ± 0.06	29.2%
+ PhaseAug	0.2202	1.012	3.600	1.095	0.9568	0.1129	3.96 ± 0.06	40.6%
MelGAN (10%)	0.2967	1.121	2.860	1.177	0.9443	0.1399	3.92 ± 0.06	31.1%
+ PhaseAug	0.2824	1.117	2.891	1.271	0.9450	0.1362	3.98 ± 0.06	43.9%
HiFi-GAN (1%)	0.3383 ± 0.003	1.177 ± 0.003	2.703 ± 0.02	1.320 ± 0.01	0.9350 ± 0.001	0.1576 ± 0.002	3.80 ± 0.05	33.5%
+ PhaseAug	0.3302 ± 0.004	1.169 ± 0.003	2.726 ± 0.04	1.314 ± 0.05	0.9363 ± 0.001	0.1543 ± 0.001	3.88 ± 0.06	43.3%
MelGAN (1%)	0.3906 ± 0.004	1.275 ± 0.002	2.020 ± 0.005	1.438 ± 0.02	0.9256 ± 0.001	0.1811 ± 0.002	3.65 ± 0.07	36.4%
+ PhaseAug	0.3756 ± 0.004	1.257 ± 0.002	2.093 ± 0.02	1.416 ± 0.05	0.9248 ± 0.002	0.1803 ± 0.002	3.56 ± 0.07	38.5%

3.3. Evaluation Metrics

To evaluate our methods, we measure mel-spectrogram mean average error (MAE), multi-resolution STFT (M-STFT) [16], 16000 Hz wide-band perceptual evaluation of speech quality (PESQ) [17], mel-cepstral distortion (MCD) [18], periodicity error [6], and F1 score of voiced/unvoiced classification (V/UV F1) [6] as objective metrics. We conduct subjective evaluation using mean opinion score (MOS) and pairwise preference test. Each of MOS is performed with 150 samples and 750 ratings, a with 95% confidence interval (CI). In the pairwise preference test, each pair is evaluated using 150 samples and 1500 votes. Participants are asked to select a preferred sample between two models, with or without PhaseAug, or a neutral option.

4. RESULTS

Table 1 denotes the results from the models trained with or without PhaseAug. Without some cases of MCD and V/UV F1, our method improves the evaluation metrics for HiFi-GAN and MelGAN generators. Especially, PhaseAug improves periodicity (average 3% decreased), which is the most important metric related to the artifacts. In addition, models with 10% dataset and PhaseAug show better MAE than models with 100% dataset and without PhaseAug. There are no statistically significant differences between MOS tests. MOS of augmented ground truth signals also do not have significant difference between ground truth signals. However, models with PhaseAug show higher preferences with significant differences without MelGAN 1% case, since 1% of dataset is not enough to train MelGAN.

5. DISCUSSION, LIMITATION, AND FUTURE WORK

In this work, we propose PhaseAug, the first differentiable augmentation for speech synthesis to overcome the discriminator overfitting and the one-to-one paired data problem. Our method rotates the phases of speech to simulate one-to-many mapping for vocoder discriminators. With PhaseAug, we could enhance the value of evaluation metrics without modifying network architectures. Since PhaseAug is also effective in limited

dataset cases, we expect that our method could be applicable during fine-tuning GAN-based vocoder with a small dataset.

While Zhao *et al.* [9] and Karras *et al.* [10] report that DiffAugment could prevent discriminator overfitting, we observe that MPD and MSD show similar accuracy patterns with or without PhaseAug. We expect that this is caused by the difference between unconditional and conditional generative models. While accuracy patterns are similar, mean of MPD outputs (closer to 0.5) are shown that MPD provides more useful information to the generator with our method. In addition, leaking of PhaseAug is negligible, since MOS of augmented signals do not have significant difference with ground truth.

We compare our method with several objective evaluation metrics. However, these metrics have limitations as they measure the difference between the generated signals and the ground truth signals in a one-to-many mapping problem. Moreover, periodicity artifact is observed in short moments, these metrics are not appropriate for evaluating it. Listeners focus on samples' global naturalness, not temporal artifact, so MOS is not an appropriate metric for it. However, pairwise test shows significant differences. We also tested our method to VITS [19], a GAN-based end-to-end text-to-speech (E2E TTS) model. However measuring objective evaluation metrics was difficult as E2E TTS is a more complex one-to-many problem than neural vocoding.

Since PhaseAug could approximate differentiable time-shift, we could train a shift-equivariant speech synthesis model by applying it to hidden latents and output of model without filtered nonlinearity [7, 20]. In addition, PhaseAug is also applicable as data augmentation to other speech synthesis models such as neural audio upsampling [21, 22], while we focus on applying it as a DiffAugment for GAN-based vocoders.

6. ACKNOWLEDGMENT

The authors would like to thank Minh Kim of MINDsLab, Jinwoo Kim and Hyeonuk Nam from KAIST, Dongho Choi and Kang-wook Kim from SNU for valuable discussions.

7. REFERENCES

- [1] Ian Goodfellow, Jean Pouget-Abadie, Mehdi Mirza, Bing Xu, David Warde-Farley, Sherjil Ozair, Aaron Courville, and Yoshua Bengio, “Generative adversarial nets,” in *NeurIPS*, 2014, pp. 2672–2680.
- [2] Kundan Kumar, Rithesh Kumar, Thibault de Boissiere, Lucas Gestein, Wei Zhen Teoh, Jose Sotelo, Alexandre de Brébisson, Yoshua Bengio, and Aaron C Courville, “MelGAN: Generative Adversarial Networks for Conditional Waveform Synthesis,” in *NeurIPS*, 2019, pp. 14910–14921.
- [3] Jinhyeok Yang, Junmo Lee, Youngik Kim, Hoon-Young Cho, and Injung Kim, “VocGAN: A High-Fidelity Real-Time Vocoder with a Hierarchically-Nested Adversarial Network,” in *Interspeech*, 2020, pp. 200–204.
- [4] Jungil Kong, Jaehyeon Kim, and Jaekyoung Bae, “HiFiGAN: Generative Adversarial Networks for Efficient and High Fidelity Speech Synthesis,” in *NeurIPS*, 2020, pp. 17022–17033.
- [5] Ji-Hoon Kim, Sang-Hoon Lee, Ji-Hyun Lee, and Seong-Whan Lee, “Fre-GAN: Adversarial Frequency-Consistent Audio Synthesis,” in *Interspeech*, 2021, pp. 2197–2201.
- [6] Max Morrison, Rithesh Kumar, Kundan Kumar, Prem Seetharaman, Aaron Courville, and Yoshua Bengio, “Chunked Autoregressive GAN for Conditional Waveform Synthesis,” in *ICLR*, 2022.
- [7] Sang gil Lee, Wei Ping, Boris Ginsburg, Bryan Catanzaro, and Sungroh Yoon, “BigVGAN: A Universal Neural Vocoder with Large-Scale Training,” *arXiv preprint arXiv:2206.04658*, 2022.
- [8] Taejun Bak, Junmo Lee, Hanbin Bae, Jinhyeok Yang, Jaesung Bae, and Young-Sun Joo, “Avocodo: Generative Adversarial Network for Artifact-free Vocoder,” *arXiv preprint arXiv:2206.13404*, 2022.
- [9] Shengyu Zhao, Zhijian Liu, Ji Lin, Jun-Yan Zhu, and Song Han, “Differentiable Augmentation for Data-Efficient GAN Training,” in *NeurIPS*, 2020, pp. 7559–7570.
- [10] Tero Karras, Miika Aittala, Janne Hellsten, Samuli Laine, Jaakko Lehtinen, and Timo Aila, “Training Generative Adversarial Networks with Limited Data,” in *NeurIPS*, 2020, pp. 12104–12114.
- [11] Min-Jae Hwang, Ryuichi Yamamoto, Eunwoo Song, and Jae-Min Kim, “TTS-by-TTS: TTS-Driven Data Augmentation for Fast and High-Quality Speech Synthesis,” in *IEEE ICASSP*, 2021, pp. 6598–6602.
- [12] Hyeon-Seok Choi, Juheon Lee, Wansoo Kim, Jie Hwan Lee, Hoon Heo, and Kyogu Lee, “Neural Analysis and Synthesis: Reconstructing Speech from Self-Supervised Representations,” in *NeurIPS*, 2021, pp. 16251–16265.
- [13] Jilong Wu, Adam Polyak, Yaniv Taigman, Jason Fong, Prabhav Agrawal, and Qing He, “Multilingual Text-To-Speech Training Using Cross Language Voice Conversion And Self-Supervised Learning Of Speech Representations,” in *IEEE ICASSP*, 2022, pp. 8017–8021.
- [14] Jong Wook Kim, Justin Salamon, Peter Li, and Juan Pablo Bello, “CREPE: A Convolutional Representation for Pitch Estimation,” in *IEEE ICASSP*, 2018, pp. 161–165.
- [15] Keith Ito and Linda Johnson, “The LJ Speech Dataset,” <https://keithito.com/LJ-Speech-Dataset/>, 2017.
- [16] Ryuichi Yamamoto, Eunwoo Song, and Jae-Min Kim, “Parallel Wavegan: A Fast Waveform Generation Model Based on Generative Adversarial Networks with Multi-Resolution Spectrogram,” in *IEEE ICASSP*, 2020, pp. 6199–6203.
- [17] A.W. Rix, J.G. Beerends, M.P. Hollier, and A.P. Hekstra, “Perceptual Evaluation of Speech Quality (PESQ): A New Method for Speech Quality Assessment of Telephone Networks and Codecs,” in *IEEE ICASSP*, 2001, pp. 749–752.
- [18] R. Kubichek, “Mel-cepstral distance measure for objective speech quality assessment,” in *IEEE PRCCSP*, 1993, pp. 125–128.
- [19] Jaehyeon Kim, Jungil Kong, and Juhee Son, “Conditional Variational Autoencoder with Adversarial Learning for End-to-End Text-to-Speech,” in *ICML*, 2021, pp. 5530–5540.
- [20] Tero Karras, Miika Aittala, Samuli Laine, Erik Härkönen, Janne Hellsten, Jaakko Lehtinen, and Timo Aila, “Alias-Free Generative Adversarial Networks,” in *NeurIPS*, 2021, pp. 852–863.
- [21] Junhyeok Lee and Seungu Han, “NU-Wave: A Diffusion Probabilistic Model for Neural Audio Upsampling,” in *Interspeech*, 2021, pp. 1634–1638.
- [22] Seungu Han and Junhyeok Lee, “NU-Wave 2: A General Neural Audio Upsampling Model for Various Sampling Rates,” in *Interspeech*, 2022, pp. 4401–4405.